

# Analyst

Accepted Manuscript



This is an *Accepted Manuscript*, which has been through the Royal Society of Chemistry peer review process and has been accepted for publication.

*Accepted Manuscripts* are published online shortly after acceptance, before technical editing, formatting and proof reading. Using this free service, authors can make their results available to the community, in citable form, before we publish the edited article. We will replace this *Accepted Manuscript* with the edited and formatted *Advance Article* as soon as it is available.

You can find more information about *Accepted Manuscripts* in the [Information for Authors](#).

Please note that technical editing may introduce minor changes to the text and/or graphics, which may alter content. The journal's standard [Terms & Conditions](#) and the [Ethical guidelines](#) still apply. In no event shall the Royal Society of Chemistry be held responsible for any errors or omissions in this *Accepted Manuscript* or any consequences arising from the use of any information it contains.

1  
2  
3  
4  
5  
6  
7  
8  
9  
10  
11  
12  
13  
14  
15  
16  
17  
18  
19  
20  
21  
22  
23  
24  
25  
26  
27  
28  
29  
30  
31  
32  
33  
34  
35  
36  
37  
38  
39  
40  
41  
42  
43  
44  
45  
46  
47  
48  
49  
50  
51  
52  
53  
54  
55  
56  
57  
58  
59  
60

# Online SERS Detection and Characterization of Eight Biologically-Active Peptides Separated by Capillary Zone Electrophoresis

Pierre Negri, Scott A. Sarver, Nicole M. Schiavone, Norman J. Dovichi, and Zachary D. Schultz\*

Department of Chemistry and Biochemistry, University of Notre Dame, Notre Dame, IN 46556

\*Corresponding Author email: Schultz.41@nd.edu

## Abstract

There is a need for low cost, sensitive and chemical specific detectors for routine characterization of biomolecules. In this study, we utilize sheath-flow surface-enhanced Raman scattering (SERS) to analyze a mixture of eight biologically-active peptides separated by capillary zone electrophoresis (CZE). Analysis of the SERS electropherogram resulting from online detection resolves the characteristic Raman bands attributed to the amino acid constituents of each peptide, which enables identification. The detection limit by SERS was found to be  $10^{-8}$  M. Our results suggest that the structural information obtained from the detected vibrational modes provides complementary characterization to other chemically specific detectors like mass spectrometry and improved chemical identification over other commonly used optical-based post-chromatographic detection methods. In addition, the sheath-flow SERS detection results in band narrowing in the observed electropherogram that enables distinction of closely migrating species. The results presented here indicate that online SERS detection can provide fast, robust, reproducible, and chemical specific detection to facilitate the characterization of peptides.

## Introduction

The identification of biomolecules has broad application in areas such as clinical diagnostics, environmental monitoring, and pharmaceutical production. In the last few decades, progress has been made toward improving separation and developing better characterization methods for a variety of complex biomolecules. Recent improvements in microcolumn separation science and more specifically the incorporation of high sensitivity detectors have allowed analysis of minute amounts of sample with reduced processing time.<sup>1</sup>

Improving separations has been a key factor for identifying biomolecules such as DNA, lipids, metabolites, amino acids, peptides and proteins in complex biological mixtures.<sup>2</sup> The most common detection method for characterizing these biomolecules is mass spectrometry (MS) due to its universality, sensitivity, and selectivity.<sup>3</sup> While mass spectrometry can provide exquisite analyte identification, the cost of high-resolution mass spectrometers typically limits this analysis to core facilities. Additionally, certain classes of molecules require complex sample derivatization, while others exhibit poor ionization and are difficult to detect.<sup>4-6</sup> Furthermore, the interface between the column and the mass spectrometer can limit the breadth of applications available for analysis.<sup>7, 8</sup>

A low cost, chemical specific detector could facilitate analysis of biomolecular samples. Optical-based detection techniques provide an appealing alternative as they are typically nondestructive and relatively inexpensive. It is quite common to use optical detectors such as UV-visible absorption or laser-induced fluorescence (LIF) to detect analytes post-separation. However, LIF requires incorporation of a fluorescent label to achieve high sensitivity.<sup>9-12</sup> And while UV-visible absorption offers a low cost and flexible alternative, it suffers from modest

1  
2  
3 sensitivity.<sup>13, 14</sup> More importantly, LIF and UV-visible absorption both lack molecular  
4  
5  
6 specificity which precludes their use for direct analyte identification.  
7  
8

9 Raman spectroscopy is an appealing optical-based detection method for post-separation  
10  
11 analysis of biomolecules. Raman detection is readily incorporated to liquid-phased separation  
12  
13 and provides label-free structural information through signals arising from vibrational modes.<sup>15-</sup>  
14  
15  
16 <sup>17</sup> Previous studies have shown that post-chromatographic Raman detection suffers from poor  
17  
18 sensitivity without sample concentration or resonance enhancement.<sup>18, 19</sup> Recently, we  
19  
20 demonstrated surface-enhanced Raman scattering (SERS) detection of rhodamine isomers and of  
21  
22 amino acids following a capillary zone electrophoresis separation.<sup>20, 21</sup> The SERS enhancement  
23  
24 enabled us to detect concentrations ranging from  $10^{-5}$  –  $10^{-10}$  M without resonant enhancement.  
25  
26  
27 The structural information provided by the SERS spectra offers a chemical specific alternative  
28  
29 for routine analysis of biomolecules.  
30  
31  
32

33 In this report, we demonstrate the ability of our sheath-flow SERS detector to  
34  
35 characterize and identify eight biologically-active peptides separated by capillary zone  
36  
37 electrophoresis (CZE). Peptides are a class of biomolecules well characterized in bioanalysis. As  
38  
39 a result, they provide an established test system to assess the sensitivity and robustness of our  
40  
41 SERS detection method. Our results demonstrate the ability of our sheath-flow SERS detector to  
42  
43 identify peptides from changes in the observed vibrational bands that correlate with the peptides'  
44  
45 amino acid composition.  
46  
47  
48  
49  
50  
51  
52  
53  
54  
55  
56  
57  
58  
59  
60

## Experimental Methods

Materials and Reagents. Lyophilized peptides were purchased from Peptides International (Louisville, KY). The peptides were dissolved in water to a concentration of 500  $\mu\text{M}$ , aliquoted and stored at  $-20^{\circ}\text{C}$ . Ammonium bicarbonate was purchased from Sigma-Aldrich (St. Louis, MO). Ultrapure water (18.2  $\text{M}\Omega\text{ cm}$ ) was obtained from a Barnstead Nanopure filtration system. All other chemicals were of analytical grade and used without any further purification.

SERS Substrate Fabrication. Silver (Ag, Sigma-Aldrich, 99.999%) was vapor deposited onto a commercial anodized aluminum oxide filter (Anodisc 13, Whatman) with 0.1  $\mu\text{m}$  pores as previously described.<sup>22</sup> Prior to deposition, the Anodisc filters were cleaned for 5 minutes in an  $\text{Ar}^+$  plasma (Model PDC-32G, Harrick Plasma, Ithaca, NY) to remove surface contamination and mounted on a substrate holder in the deposition chamber. Silver was deposited at a constant rate of 1.0-1.5  $\text{\AA}/\text{s}$  until a quartz crystal microbalance (QCM) registered a final nominal thickness of 500 nm. Following deposition, the substrates were allowed to cool to room temperature under vacuum inside the deposition chamber for 30 minutes. Prior to use, the SERS-active substrates were stored under vacuum to prevent oxidation and surface contamination.

CZE-SERS Setup. SERS-active substrates were integrated into a custom-built flow cell, as previously described.<sup>23</sup> A 50 cm (72  $\mu\text{m}$  i.d., 143  $\mu\text{m}$  o.d.) uncoated fused silica capillary (Polymicro Technologies, Phoenix, AZ) was used. When selecting the capillary, our previous work shows that a thin capillary wall thickness is important for efficient hydrodynamic focusing. The distal end of the separation capillary was placed in a sheath-flow channel that was defined by a 250  $\mu\text{m}$  thick silicone gasket with a 2 mm slit, covered with a standard cover glass that was held in place by the stainless steel top plate. The proximal end of the capillary was inserted into a

1  
2  
3 custom-made injection block.<sup>24</sup> A syringe pump (Model NE-500 OEM, New Era Pump Systems  
4 Inc., Farmingdale, NY) controlled by LabView (National Instruments, Austin, TX) was used to  
5 pump the sheath liquid (10 mM ammonium bicarbonate buffer, pH 8) at a rate of 10  $\mu\text{L}/\text{min}$ ,  
6  
7  
8 which provided hydrodynamic focusing of the sample into the detection region.  
9  
10  
11

12  
13  
14 CZE was performed in positive mode by applying a constant potential of 15 kV to the Pt  
15 electrode embedded in the custom-built injection block using a Spellman, CZE 1000R power  
16 supply (Spellman High Voltage Electronics Corp., Hauppauge, NY). The system was grounded  
17 directly from the SERS substrate during the CZE separations. Sample injection was performed  
18 using a 2 s pressure injection, which introduced  $\sim 34$  nL of sample into the capillary. Following  
19 injection, the sample was replaced with 10 mM ammonium bicarbonate buffer (pH 8) in the  
20 injection block and 15 kV ( $\sim 15$   $\mu\text{A}$ ,  $300$   $\text{V cm}^{-1}$ ) was applied to the Pt electrode at the sample  
21 end of the capillary.  
22  
23  
24  
25  
26  
27  
28  
29  
30  
31

32 Raman spectra were collected using a previously described home-built Raman  
33 microscope.<sup>22</sup> Excitation was provided by a 632.8 nm HeNe laser beam that was directed into the  
34 flow chamber using a 40X water-immersion objective (Olympus, NA = 0.8), resulting in a spot  
35 size of approximately  $0.4$   $\mu\text{m}^2$ . The laser power at the sample was attenuated to 1 mW. Raman  
36 back-scattering was collected by the same objective lens and directed to the Czerny-Turner  
37 spectrograph (Andor) and EMCCD (Newton 970, Andor). SERS spectra between 2000 and 500  
38  $\text{cm}^{-1}$  were recorded in kinetic series with 200 ms acquisition times. The spectral resolution of the  
39 home-built Raman instrument is  $3$   $\text{cm}^{-1}$  based on the grating (600 grooves/mm), entrance slit (25  
40  $\mu\text{m}$ ), monochromator pathlength (320 mm), and CCD pixel size.  
41  
42  
43  
44  
45  
46  
47  
48  
49  
50  
51  
52  
53  
54  
55  
56  
57  
58  
59  
60

1  
2  
3 *SERS Data Analysis.* Band height and peak frequency determination were performed using  
4  
5 MATLAB (R2012a, The Mathworks Inc., Natwick, MA). Baseline correction (Weighted Least  
6  
7 Squares, basic filter, 2<sup>nd</sup> order) and data smoothing (Savitsky-Golay, 3 points, 0<sup>th</sup> order) were  
8  
9 performed on the SERS electropherograms using PLS Toolbox version 6.2 (Eigenvector  
10  
11 Research Inc., Wenatchee, WA) in MATLAB. The SERS electropherogram was created by  
12  
13 plotting the Raman intensity on the z-axis as a function of Raman shift on the y-axis and  
14  
15 migration time along the x-axis. The total photon electropherogram (TPE) was plotted by adding  
16  
17 all the photons detected at all Raman shifts during each acquisition as a function of migration  
18  
19 time.  
20  
21  
22  
23  
24

## 25 **Results and Discussion**

26  
27  
28  
29  
30  
31  
32  
33  
34  
35  
36  
37  
38  
39  
40  
41  
42  
43  
44  
45  
46  
47  
48  
49  
50  
51  
52  
53  
54  
55  
56  
57  
58  
59  
60

Eight biologically-active peptides were chosen to assess the detection capability and sensitivity of our sheath-flow SERS detector. To study the amino acid contribution in the observed SERS signal, the peptides were chosen to have different combinations of aromatic and sulfur-containing amino acids, including two peptides containing a single amino acid polymorphism (Angiotensin II and Angiotensin III). The peptides range in mass from MW=593.68 (Laminin Pentapeptide) to 1637.9 (Somatostatin). The isoelectric points vary from 7.19 (Angiotensin II) to 11.12 (Substance P). The peptide mixture was prepared in 10 mM ammonium bicarbonate buffer (pH 8), where the concentration of each peptide is 50  $\mu$ M. Table 1 summarizes the properties of the peptides used in this study.

Figure 1A shows the SERS electropherogram resulting from the separation and online detection of the peptide mixture. The electropherogram shows signals associated with the peptides at  $t_{m1} = 274 \pm 6$  s,  $t_{m2} = 300 \pm 11$  s,  $t_{m3} = 328 \pm 9$  s,  $t_{m4} = 332 \pm 8$  s,  $t_{m5} = 380 \pm 13$  s,  $t_{m6}$

1  
2  
3 =  $389 \pm 6$  s,  $t_{m7} = 395 \pm 13$  s, and  $t_{m8} = 430 \pm 15$  s. Analysis of Figure 1A shows that each  
4  
5  
6  
7  
8  
9  
10  
11  
12  
13  
14  
15  
16  
17  
18  
19  
20  
21  
22  
23  
24  
25  
26  
27  
28  
29  
30  
31  
32  
33  
34  
35  
36  
37  
38  
39  
40  
41  
42  
43  
44  
45  
46  
47  
48  
49  
50  
51  
52  
53  
54  
55  
56  
57  
58  
59  
60

=  $389 \pm 6$  s,  $t_{m7} = 395 \pm 13$  s, and  $t_{m8} = 430 \pm 15$  s. Analysis of Figure 1A shows that each analyte is very well resolved. The observed migration peak widths vary from 0.5 to 1.5 s, as seen in to the total photon electropherogram (TPE) shown in Figure 1B. Similar to the total ion count commonly plotted in separations with MS detection, the total photon count helps characterize peptide migration.

We performed CZE-ESI-MS to confirm the identity, the elution order and the migration times of the peptides observed in the CZE-SERS experiments. CZE-ESI-MS has been used extensively for the study of peptides and proteins.<sup>25-28</sup> Figure S1 in the ESI shows the total (A) and extracted (B) ion (MS) electropherograms of the same peptide mixture resulting from the CZE-ESI-MS experiments following a 1:10 dilution such that the concentration of each peptide is  $5.0 \times 10^{-6}$  M. The capillary dimensions and separation buffer composition were kept identical to those used in the optimized SERS experiments to provide a direct comparison. As seen in Figure S1, the CZE-ESI-MS experiments detected Laminin Pentapeptide ( $m/z = 594.3367$ ) at  $t_{m1} = 318$  s, Bombesin ( $m/z = 810.4175$ ) at  $t_{m2} = 324$  s, Angiotensin III ( $m/z = 466.2615$ ) at  $t_{m3} = 361$  s, Amyloid  $\beta$ -Protein ( $m/z = 530.7956$ ) at  $t_{m4} = 367$  s, Somatostatin ( $m/z = 819.3678$ ) at  $t_{m5} = 378$  s, Angiotensin I ( $m/z = 648.8478$ ) at  $t_{m6} = 388$  s, Angiotensin II ( $m/z = 523.775$ ) at  $t_{m7} = 391$  s and Substance P ( $m/z = 674.3733$ ) at  $t_{m8} = 695$  s. The advantage of MS detection is that it provides unambiguous identification of the known peptides based on accurate mass to charge ratios. Figure S2 in the ESI shows the MS spectra of the eight detected peptides. Table S1 in the ESI summarizes the results of the CZE-ESI-MS experiment and lists each peptide detected, along with the observed  $m/z$ , predicted  $m/z$ , and sample concentration.

We investigated the sensitivity of the SERS detector by performing CZE-SERS using varying concentrations of Angiotensin I. The separation and detection conditions were kept

1  
2  
3 identical to those previously described. Figure 2 shows the averaged SERS spectra resulting from  
4 the detection of Angiotensin I at concentrations ranging from 50  $\mu\text{M}$  to 50 nM. The high degree  
5 of spectral similarity of the SERS spectra of Angiotensin I shown in Figure 2 demonstrates the  
6 reproducibility and robustness of our sheath-flow SERS detector. As expected, the Raman signal  
7 decreases with decreasing analyte concentration. Figure 2 shows that Angiotensin I was detected  
8 at 50 nM (orange trace). The observed signal at 50 nM is just above the noise level (green trace),  
9 suggesting this concentration is near the detection limit.  
10  
11  
12  
13  
14  
15  
16  
17  
18  
19

20  
21 The SERS electropherogram shown in Figure 1A resolves all eight peptides. The total  
22 ion count electropherogram in Figure S1A shows co-migration of many of the peptides in the  
23 CZE-ESI-MS experiments. The inset in Figure 2 shows the area of the Angiotensin I amide II  
24 band at 1547  $\text{cm}^{-1}$  as a function of increasing concentration. The plot exhibits the Langmuir-type  
25 behavior typical of SERS. This observation is consistent with our previous findings showing that  
26 hydrodynamic focusing promotes molecule confinement at the silver surface, which enhances the  
27 physical interaction with the SERS substrate.<sup>23</sup> As a result, the SERS signal is observed from the  
28 portion of the migrating analyte band with sufficient concentration to promote adsorption,<sup>29</sup>  
29 which narrows the observed width of the migration peak. Figure 3 shows the change in  
30 migration peak width determined from the 1547  $\text{cm}^{-1}$  band of Angiotensin I with increasing  
31 concentration. As the concentration exceeds the critical value for adsorption, the width of the  
32 peaks is observed to increase. This increase in migration peak width corresponds to the  
33 concentration of analyte in the migration band sufficient to promote adsorption. This agrees with  
34 other results where SERS signals in solution were correlated with adsorbed molecules.<sup>30</sup> The  
35 dependence on Langmuir-type adsorption implies a nonlinear response that results in peak  
36 narrowing, which provides improved separation resolution. This peak-narrowing is valuable for  
37  
38  
39  
40  
41  
42  
43  
44  
45  
46  
47  
48  
49  
50  
51  
52  
53  
54  
55  
56  
57  
58  
59  
60

1  
2  
3 resolving co-migrating species. Furthermore, sample pre-concentration techniques, such as  
4  
5 isotachopheresis that have been used with MS detection,<sup>31</sup> may also improve SERS detection.  
6  
7

8  
9 Figure 4 shows the averaged SERS spectra of each of the eight peptides extracted from  
10  
11 the SERS electropherogram shown in Figure 1A. Although SERS spectra provide structural  
12  
13 information in the form of bands arising from bond vibrations, it is difficult to unambiguously  
14  
15 identify the peptides on the basis of the SERS spectra alone. As expected based on the peptides'  
16  
17 composition, the SERS spectra shown in Figure 4 share a high degree of similarity. Notably,  
18  
19 characteristic vibrations of the amine and carboxyl groups are present in each spectrum,  
20  
21 suggesting that charged groups are interacting with the silver SERS surface. However, the amino  
22  
23 acid constituents in each peptide give rise to unique spectral features that enable differentiation.  
24  
25  
26  
27

28  
29 Spectral analysis of the SERS data provides chemical insight into the detected peptides.  
30  
31 Figure 4a shows the averaged SERS spectrum of Laminin Pentapeptide extracted from the SERS  
32  
33 electropherogram shown in Figure 1A between  $t = 273.6$  and  $274.4$  s. Table S2 in the ESI  
34  
35 summarizes the observed bands and their assignments in the SERS spectrum of Laminin  
36  
37 Pentapeptide. The presence of the two distinct vibrations intrinsic to Tyr and the absence of other  
38  
39 aromatic features (Phe or Trp) support the identification of this peptide as Laminin Pentapeptide.  
40  
41 Other peptides containing tyrosine also contain other aromatic amino acids, which tend to have  
42  
43 distinct SERS signals. Other vibrational bands common to peptides are also observed.  
44  
45  
46  
47

48  
49 Figure 4b shows the SERS spectrum of Bombesin extracted from the SERS  
50  
51 electropherogram (Figure 1A) between  $t = 302.4$  and  $303.0$  s. Table S3 in the ESI summarizes  
52  
53 the observed bands in the SERS spectrum of Bombesin shown in Figure 4b along with their  
54  
55 literature assignments. The SERS spectrum is characterized by unique bands that can be directly  
56  
57  
58  
59  
60

1  
2  
3 assigned to the vibrations of aromatic and sulfur-containing amino acids. We assign the band at  
4  
5 674  $\text{cm}^{-1}$  to the characteristic C-S stretching vibration of Met.<sup>32,33</sup> The band at 1547  $\text{cm}^{-1}$  is  
6  
7 attributed to the indole vibration of Trp.<sup>34-37</sup> These two distinct bands are unique to Bombesin,  
8  
9 the only peptide in the mixture to contain Met and Trp. In addition, the  $\text{CH}_3$  symmetric and  
10  
11 asymmetric bending modes observed at 1344 and 1481  $\text{cm}^{-1}$  can be assigned to the methyl group  
12  
13 in pyruvic acid at the N-terminus of Bombesin.<sup>38</sup>  
14  
15  
16  
17

18  
19 The SERS spectrum of Angiotensin III is shown in Figure 4c, extracted from Figure 1A  
20  
21 between  $t = 328.2$  and  $330.0$  s. The main bands present in the SERS spectrum of Angiotensin III  
22  
23 are tabulated in Table S4 in the ESI, along with band assignments to particular vibrational  
24  
25 modes. The SERS spectrum shows distinct bands characteristic of Tyr and Phe found in the  
26  
27 sequence of all the Angiotensins. These features include the bands at 854 (Fermi resonance  
28  
29 between ring breathing and out-of-plane ring bending overtone of Tyr),<sup>37,39</sup> 1204 (combined ring  
30  
31 breathing mode of Phe and  $\text{C}_\beta\text{-C}_\gamma$  stretching mode of Tyr),<sup>34,36,40</sup> 1288 (imidazole C-H in-plane  
32  
33 bending),<sup>41</sup> 1482 (combined imidazole ring stretching and imidazole  $\text{C}_1\text{-H}$  in plane bending),<sup>42</sup>  
34  
35 and 1602  $\text{cm}^{-1}$  (ring C-C stretching of Phe).<sup>43</sup>  
36  
37  
38  
39

40  
41 Figure 3d shows the SERS spectrum of Somatostatin extracted from the SERS  
42  
43 electropherogram (Figure 1A) between  $t = 332.6$  and  $333.4$  s. Table S5 in the ESI summarizes  
44  
45 the observed bands in the SERS spectrum of Somatostatin, along with their literature  
46  
47 assignments. The presence of the C-S stretching mode of cysteine and bands attributed to the  
48  
49 aromatic constituents (Phe and Trp) are observed. Somatostatin is reported to form a disulfide  
50  
51 bond ( $\text{Cys}^3\text{-Cys}^{14}$ ). While sulfur is known to have a strong affinity for silver, the S-S vibration  
52  
53 typically present around 530  $\text{cm}^{-1}$  is not observed. This could indicate the bond is cleaved or  
54  
55 oriented parallel to the SERS substrate where it would not be observed. The only spectral  
56  
57  
58  
59  
60

1  
2  
3 contribution from the disulfide bond is the C-S stretching mode observed as a sharp band at 674  
4  
5  $\text{cm}^{-1}$ .  
6  
7

8  
9 The SERS spectrum of Amyloid  $\beta$  is shown in Figure 4e, extracted from Figure 1A  
10  
11 between 381.0 and 381.8 s. A complete table of the observed bands in the SERS spectrum of  
12  
13 Amyloid  $\beta$ -Protein and their assignments is provided in Table S6 in the ESI. The absence of  
14  
15 bands attributed to characteristic aromatic vibrations and the presence of the band attributed to  
16  
17 the C-S stretching vibration at  $674 \text{ cm}^{-1}$  provide spectral evidence for identification of this  
18  
19 peptide as Amyloid  $\beta$ -Protein since it is the only peptide in the mixture that does not contain any  
20  
21 aromatic constituents and that possesses a Met group at the end of the peptide chain.  
22  
23  
24  
25

26  
27 Figure 4f and 4g show the averaged SERS spectra of Angiotensin I and Angiotensin II,  
28  
29 respectively, which migrate closely. The Raman signals from these two peptides were extracted  
30  
31 from the SERS electropherogram in Figure 1A between  $t = 389.4$  and  $390.4$  s and  $t = 395.2$  and  
32  
33  $396.0$  s, for Angiotensin I and Angiotensin II, respectively. Tables S7 and S8 in the ESI  
34  
35 summarize the observed bands in the SERS spectra along with their literature assignments. The  
36  
37 SERS spectra show a high degree of similarity, as expected by their structural similarity.  
38  
39 However, as seen in Figure 4f and 4g, many bands at the same frequency are observed to vary in  
40  
41 relative intensity, suggesting that identical molecular constituents provide different scattering  
42  
43 intensities based on minor differences in molecular composition. However, the spectra present  
44  
45 some spectral variations that allow differentiation and further identification of the peptides.  
46  
47  
48  
49

50  
51 Substance P is the last peptide to migrate off the capillary. Although near the noise in the  
52  
53 MS results, the averaged SERS spectrum is readily detected as shown in Figure 4h. The SERS  
54  
55 spectrum was extracted from the heatmap shown in Figure 1A between  $t = 427.2$  and  $428.6$  s.  
56  
57  
58  
59  
60

1  
2  
3 The SERS spectrum shows distinct bands characteristic of aromatic vibrations. The main bands  
4 present in the SERS spectrum of Substance P shown in Figure 3h are tabulated and assigned in  
5  
6 Table S9 in the ESI. The observed bands arise from the expected aromatic and hydrocarbon  
7  
8 amino acid chains based on the peptide's sequence.  
9  
10

11  
12  
13 The CZE-SERS and CZE-ESI-MS experiments generated identical elution order and  
14  
15 equivalent migration times using identical capillary conditions and buffer composition. The  
16  
17 advantage of MS detection is that an accurate mass provides unambiguous identification of the  
18  
19 known peptides. However, little additional information about the chemical nature of the peptide  
20  
21 is provided by the MS spectrum. As demonstrated in this study, the SERS spectra of the analytes  
22  
23 can be used for identification. A significant advantage of the sheath-flow SERS detector is the  
24  
25 reproducible SERS spectra obtained from analytes, something that has been problematic in other  
26  
27 SERS based detection schemes. Figure 5 illustrates the hierarchical cluster analysis (HCA)  
28  
29 dendrogram based on the thirty-five 200 ms SERS spectra extracted from the SERS  
30  
31 electropherogram shown in Figure 1A. The spectra of the peptides were clustered based on  
32  
33 Ward's linkage method for minimizing variance.<sup>44</sup> The vertical bars in the dendrogram specify  
34  
35 which spectra and classes are linked, while the horizontal bars represent the distance between the  
36  
37 linked classes. The dendrogram shown in Figure 5 demonstrates that HCA classified the SERS  
38  
39 spectra of the eight peptides into eight distinct clusters with 100% accuracy, showing the  
40  
41 robustness of HCA classification for differentiation of SERS spectra of different peptides.  
42  
43 Interestingly, Angiotensin I, Angiotensin II and Angiotensin III, which are derived from the  
44  
45 same protein, combine to form one higher order cluster. This observation demonstrates that  
46  
47 cluster analysis is able to distinguish the spectral differences between SERS spectra of closely-  
48  
49 related peptides, including single amino acid polymorphism (Angiotensin II and III). This result  
50  
51  
52  
53  
54  
55  
56  
57  
58  
59  
60

1  
2  
3 suggests that biochemical variations, such as post-translational modifications, may be detectable  
4  
5 by SERS and linked to known, previously identified sequences.  
6  
7

## 8 9 **Conclusion**

10  
11 We have demonstrated the ability of our sheath-flow SERS detector to characterize and  
12 identify eight biologically-active peptides separated by CZE. CZE-ESI-MS was used to confirm  
13 the identity, the elution order and the migration times of the peptides observed in the CZE-SERS  
14 experiments. The reproducible SERS results obtained provide a chemical specific signature that,  
15 once defined, can also be used for identification. More specifically, our sheath-flow SERS  
16 detector appears to be sensitive to the characteristic functional groups of aromatic and sulfur-  
17 containing amino acids, as well as the amine, carboxyl, and side chain constituents located at the  
18 N- and C-terminus of the peptides. The SERS assay has a limit of detection of  $10^{-8}$  M. This limit  
19 of detection appears to be limited by the Langmuir adsorption behavior. Hierarchical clustering  
20 analysis of the SERS spectra can be used to identify differences in the molecular composition of  
21 closely-related analytes.  
22  
23  
24  
25  
26  
27  
28  
29  
30  
31  
32  
33  
34  
35  
36  
37  
38

39 Classic molecular characterization consists of combining orthogonal detection methods.  
40 Here we present the use of our sheath-flow SERS detector with capillary zone electrophoresis  
41 (CZE) for trace molecule characterization in solution. The implementation of this robust,  
42 sensitive and high throughput sheath-flow SERS detector is shown to provide complementary  
43 characterization to mass spectrometry and improved chemical identification of complex  
44 biomolecular mixtures over other commonly used post-chromatographic detection methods for  
45 analytes with high biochemical relevance.  
46  
47  
48  
49  
50  
51  
52  
53  
54  
55  
56  
57  
58  
59  
60

1  
2  
3 **Acknowledgments:** The University of Notre Dame, NIH Award R21 GM107893 (ZDS), and the  
4  
5 Cottrell Scholar Award from the Research Corporation for Science Advancement (ZDS)  
6  
7 supported this work. We thank Liangliang Sun for helpful suggestions with the CZE-ESI-MS  
8  
9 experiments.  
10  
11

12  
13 **Electronic Supporting Information (ESI) available:** Supporting figures S1 and S2 show the  
14  
15 total and extracted ion electropherograms as well as the MS spectra of the eight peptides  
16  
17 resulting from the CZE-ESI-MS experiments. Supporting tables S1-S9 summarize the results  
18  
19 from the CZE-ESI-MS experiments as well as spectral assignments observed in the SERS  
20  
21 spectra of the peptides.  
22  
23  
24  
25  
26  
27  
28  
29  
30  
31  
32  
33  
34  
35  
36  
37  
38  
39  
40  
41  
42  
43  
44  
45  
46  
47  
48  
49  
50  
51  
52  
53  
54  
55  
56  
57  
58  
59  
60

**Table 1.** Peptide name (listed in alphabetical order), molecular weight, one letter amino acid sequence, and pI for the eight biologically-active peptides used in this study. The red letters in the amino acid sequence indicate aromatic and sulfur-containing amino acids.

Name	M.W	One Letter Sequence	pI
Amyloid $\beta$ -Protein	1060.3	GSNKGAIIGLM	8.88
Angiotensin I	1296.5	DRVYIHPFHL	7.38
Angiotensin II	1046.2	DRVYIHPF	7.19
Angiotensin III	931.09	RVYIHPF	9.06
Bombesin	1619.9	Pyr-QRLGNQWAVGHLM	10
Laminin Pentapeptide	593.68	YIGSR-NH <sub>2</sub>	8.88
Somatostatin	1637.9	AGCKNFFWKTFTSC (Disulfide bridge between Cys <sup>3</sup> -Cys <sup>14</sup> )	8.59
Substance P	1347.6	RPKPQQFFGLM	11.12

## Figure Caption

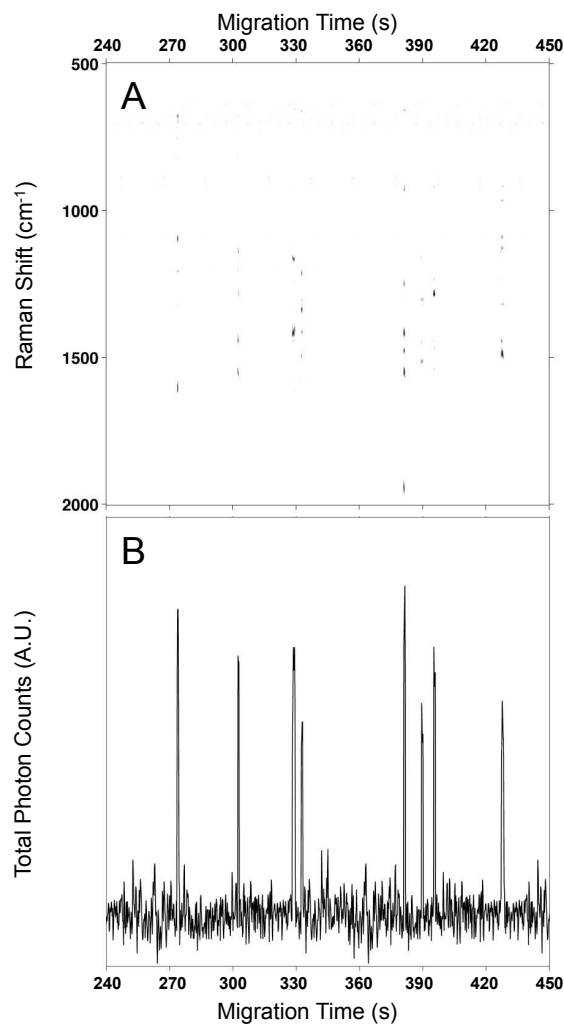


**Figure 1.** (A) The electropherogram shows the observed SERS intensity at each Raman shift as a function of migration time for the electrophoretic separation of the eight biologically-active peptides. The SERS signals indicate that Laminin Pentapeptide migrates at  $t_{m1} = 273 \pm 6$  s, Bombesin at  $t_{m2} = 302 \pm 11$  s, Angiotensin III at  $t_{m3} = 328 \pm 9$  s, Somatostatin at  $t_{m4} = 332 \pm 8$  s, Amyloid  $\beta$  -Protein at  $t_{m5} = 381 \pm 13$ s, Angiotensin I at  $t_{m6} = 389 \pm 6$  s, Angiotensin II at  $t_{m7} = 395 \pm 13$  s, and Substance P at  $t_{m8} = 427 \pm 15$  s. (B) Total photon electropherogram (TPE) extracted from (A) showing the photons detected at all Raman shifts as a function of migration time.

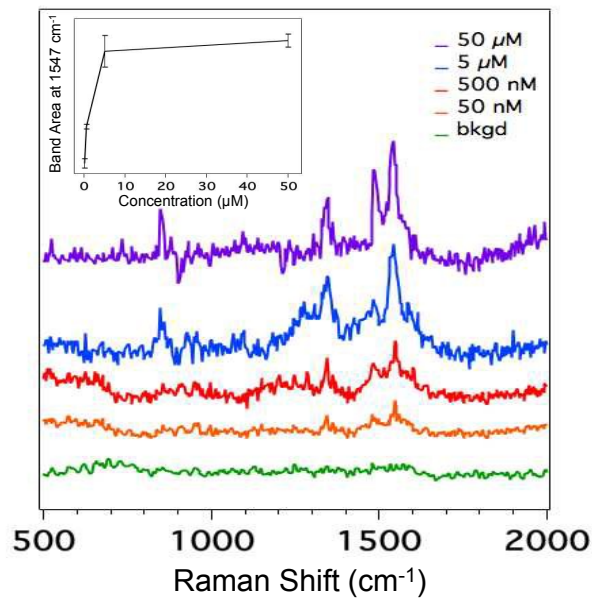


**Figure 2.** Averaged SERS spectra of Angiotensin I at concentrations ranging from 50 μM to 50 nM. The inset in Figure 4 (plotted in a linear scale) is a plot of the area of the band at 1547 cm<sup>-1</sup> assigned to the amide II vibration as a function of Angiotensin I concentration. Error bars in the inset represent the standard deviation.

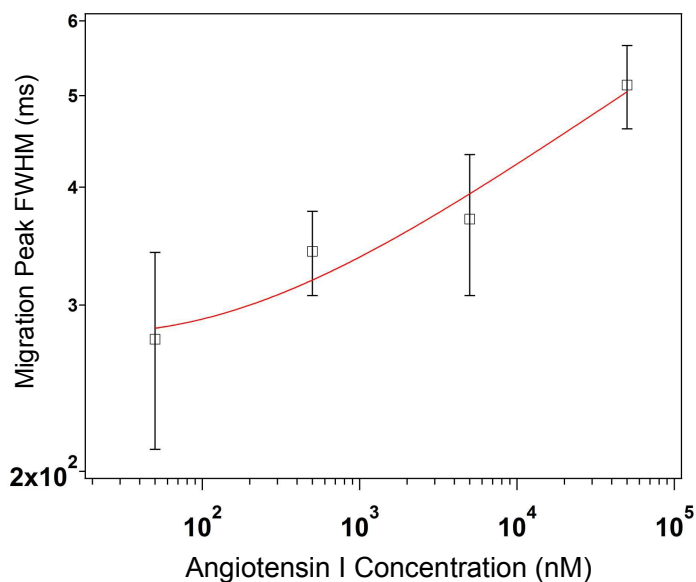


**Figure 3.** Log-log plot of the FWHM of the migration peak determined from the  $1547 \text{ cm}^{-1}$  band of Angiotensin I as a function of concentration in the range from 50 to 50,000 nM. The red trace represents the log fit. The FWHM values were extracted from the SERS electropherograms for each concentration from the data shown in Figure 3. Error bars represent the standard deviation.

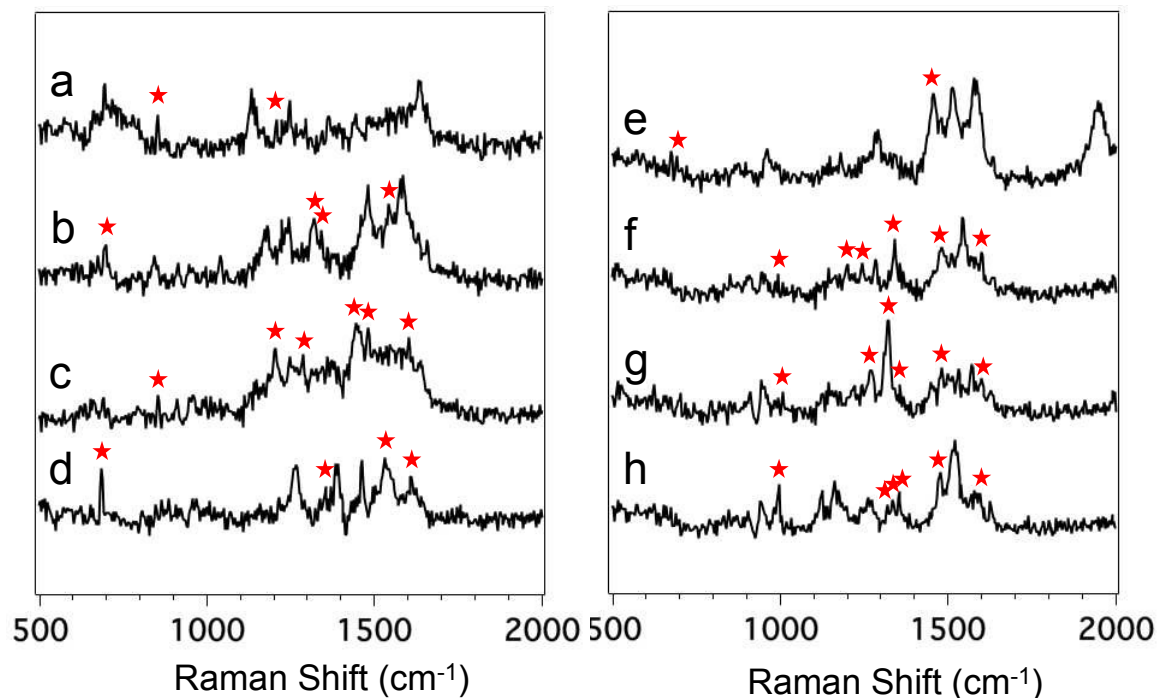


**Figure 4.** Averaged SERS spectra of (a) Laminin Pentapeptide extracted from Figure 1A between  $t = 273.6$  and  $274.4$  s, (b) Bombesin between  $t = 302.4$  and  $303.0$  s, (c) Angiotensin III between  $t = 328.2$  and  $330.0$  s, (d) Somatostatin between  $t = 332.6$  and  $333.4$  s, (e) Amyloid  $\beta$ -Protein between  $381.0$  and  $381.8$  s, (f) Angiotensin I between  $t = 389.4$  and  $390.4$  s, (g) Angiotensin II between  $t = 395.2$  and  $396.0$  s, and (h) Substance P between  $t = 427.2$  and  $428.6$  s. Red asteriks mark the bands indicative of aromatic, sulfur-containing, or side chain vibrations that enabled differentiation and identification of the eight peptides.

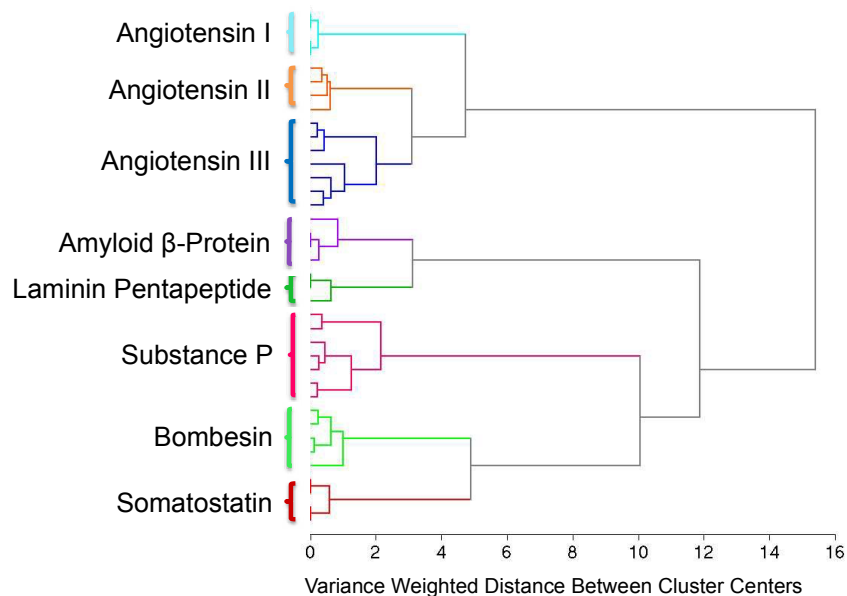


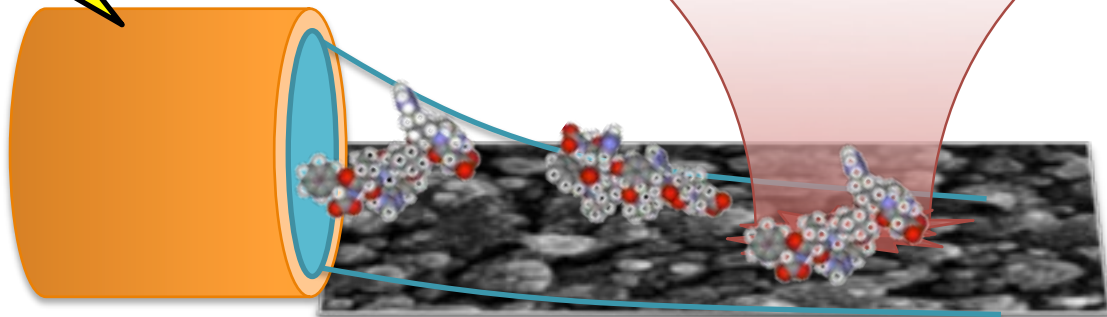
**Figure 5.** Dendrogram produced by hierarchical cluster analysis (HCA) of the SERS spectra extracted from the electropherogram shown in Figure 1A using Ward's method. A total of 35 SERS spectra extracted from the electropherogram shown in Figure 1A were used to generate this dendrogram.

## References

1. C. Legido-Quigley, N. D. Marlin, V. Melin, A. Manz and N. W. Smith, *Electrophoresis*, 2003, **24**, 917-944.
2. P.-Å. Albertsson, *Partition of cell particles and macromolecules : seperation and purification of biomolecules, cell organelles, membranes, and cells in aqueous polymer two-phase systems and their use in biochemical analysis and biotechnology*, 3rd Edition edn., New York, 1986.
3. I. A. Kaltashov and S. J. Eyles, *Mass Spectrometry Reviews*, 2002, **21**, 37-71.
4. J. F. Banks, *Electrophoresis*, 1997, **18**, 2255-2266.
5. D. Figeys and R. Aebersold, *Electrophoresis*, 1998, **19**, 885-892.
6. A. von Brocke, G. Nicholson and E. Bayer, *Electrophoresis*, 2001, **22**, 1251-1266.
7. R. D. Smith, J. A. Olivares, N. T. Nguyen and H. R. Udseth, *Analytical Chemistry*, 1988, **60**, 436-441.
8. P. Kebarle and L. Tang, *Analytical Chemistry*, 1993, **65**, A972-A986.
9. D. Y. Chen and N. J. Dovichi, *Journal of Chromatography B-Biomedical Applications*, 1994, **657**, 265-269.
10. C. E. MacTaylor and A. G. Ewing, *Electrophoresis*, 1997, **18**, 2279-2290.
11. S. Santesson, M. Andersson, E. Degerman, T. Johansson, J. Nilsson and S. Nilsson, *Analytical Chemistry*, 2000, **72**, 3412-3418.
12. K. Otsuka, K. Karuhaka, M. Higashimori and S. Terabe, *Journal of Chromatography A*, 1994, **680**, 317-320.
13. W. Beck and H. Engelhardt, *Chromatographia*, 1992, **33**, 313-316.
14. J. Z. Song, D. P. Huang, S. J. Tian and Z. P. Sun, *Electrophoresis*, 1999, **20**, 1850-1855.
15. C. Y. Chen and M. D. Morris, *Applied Spectroscopy*, 1988, **42**, 515-518.
16. K. Kneipp, H. Kneipp, I. I, R. R. Dasari and M. S. Feld, *Chemical Reviews*, 1999, **99**, 2957-2976.
17. M. Moskovits, *Reviews of Modern Physics*, 1985, **57**, 783-826.
18. K. Swinney and D. J. Bornhop, *Electrophoresis*, 2000, **21**, 1239-1250.
19. C. Y. Chen and M. D. Morris, *Journal of Chromatography*, 1991, **540**, 355-363.
20. P. Negri, R. J. Flaherty, O. O. Dada and Z. D. Schultz, *Chemical Communications*, 2014, **50**, 2707-2710.
21. P. Negri and Z. D. Schultz, *Analyst*, 2014 IN PRESS.
22. S. M. Asiala and Z. D. Schultz, *Analyst*, 2011, **136**, 4472-4479.
23. P. Negri, K. T. Jacobs, O. O. Dada and Z. D. Schultz, *Anal Chem*, 2013, **85**, 10159-10166.
24. S. N. Krylov, D. A. Starke, E. A. Arriaga, Z. Zhang, N. W. Chan, M. M. Palcic and N. J. Dovichi, *Anal Chem*, 2000, **72**, 872-877.
25. J. B. Fenn, M. Mann, C. K. Meng, S. F. Wong and C. M. Whitehouse, *Mass Spectrometry Reviews*, 1990, **9**, 37-70.
26. H. J. Issaq, *Electrophoresis*, 2001, **22**, 3629-3638.
27. R. Aebersold and D. R. Goodlett, *Chemical Reviews*, 2001, **101**, 269-295.
28. R. Aebersold and M. Mann, *Nature*, 2003, **422**, 198-207.
29. H. J. Lee, Y. Li, A. W. Wark and R. M. Corn, *Analytical Chemistry*, 2005, **77**, 5096-5100.
30. S. M. Asiala and Z. D. Schultz, *Analytical Chemistry*, 2014, **86**, 2625-2632.
31. M. Larsson and E. S. M. Lutz, *Electrophoresis*, 2000, **21**, 2859-2865.

- 1
  - 2
  - 3
  - 4
  - 5
  - 6
  - 7
  - 8
  - 9
  - 10
  - 11
  - 12
  - 13
  - 14
  - 15
  - 16
  - 17
  - 18
  - 19
  - 20
  - 21
  - 22
  - 23
  - 24
  - 25
  - 26
  - 27
  - 28
  - 29
  - 30
  - 31
  - 32
  - 33
  - 34
  - 35
  - 36
  - 37
  - 38
  - 39
  - 40
  - 41
  - 42
  - 43
  - 44
  - 45
  - 46
  - 47
  - 48
  - 49
  - 50
  - 51
  - 52
  - 53
  - 54
  - 55
  - 56
  - 57
  - 58
  - 59
  - 60
32. M. Rycenga, J. M. McLellan and Y. N. Xia, *Chemical Physics Letters*, 2008, **463**, 166-171.
33. T. Watanabe and H. Maeda, *Journal of Physical Chemistry*, 1989, **93**, 3258-3260.
34. R. P. Rava and T. G. Spiro, *Journal of the American Chemical Society*, 1984, **106**, 4062-4064.
35. T. Miura, H. Takeuchi and I. Harada, *Biochemistry*, 1991, **30**, 6074-6080.
36. F. Wei, D. M. Zhang, N. J. Halas and J. D. Hartgerink, *Journal of Physical Chemistry B*, 2008, **112**, 9158-9164.
37. E. Smith and G. Dent, *Modern Raman Spectroscopy: A Practical Approach*, Wiley, 2005.
38. S. Stewart and P. M. Fredericks, *Spectrochimica Acta Part a-Molecular and Biomolecular Spectroscopy*, 1999, **55**, 1615-1640.
39. M. N. Siamwiza, R. C. Lord, M. C. Chen, T. Takamatsu, I. Harada, H. Matsuura and T. Shimanouchi, *Biochemistry*, 1975, **14**, 4870-4876.
40. I. R. Nabiev, S. D. Trakhanov, E. S. Efremov, V. V. Marinyuk and R. M. Lasorenkomanevich, *Bioorganicheskaya Khimiya*, 1981, **7**, 941-945.
41. H. Takeuchi, N. Watanabe, Y. Satoh and I. Harada, *Journal of Raman Spectroscopy*, 1989, **20**, 233-237.
42. S. Martusevicius, G. Niaura, Z. Talaikyte and V. Razumas, *Vibrational Spectroscopy*, 1996, **10**, 271-280.
43. D. Naumann, *Applied Spectroscopy Reviews*, 2001, **36**, 239-298.
44. K. R. Beebe, R. J. Pell and M. B. Seasholtz, *Chemometrics: A Practical Guide*, New York, 1998.

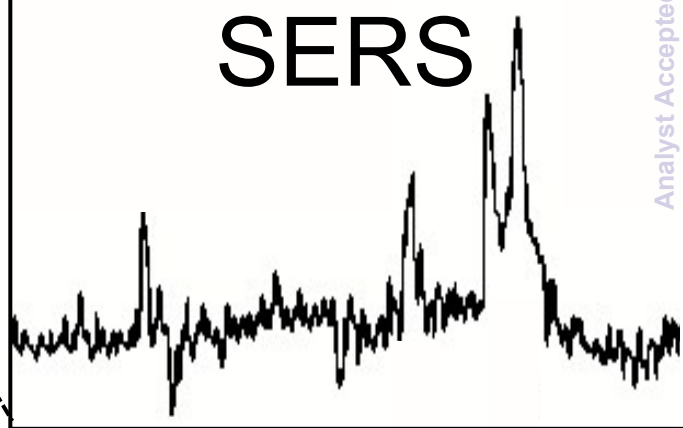
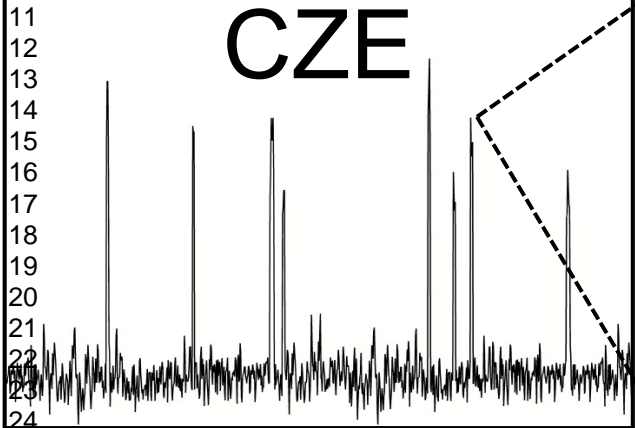
Analyst



1  
2  
3  
4  
5  
6  
7  
8  
9  
10

CZE

SERS



Migration Time

Raman Shift

25  
26